processes

MDPI

Article

Evaluation of Technical Feasibility of Solar Heat Integration in Agri-Food Industries

Julio Guillen-Angel * and Ignacio Julian *

CIRCE–Technology Centre, 50018 Zaragoza, Spain
* Correspondence: jguillen@fcirce.es (J.G.-A.); iajulian@fcirce.es (I.J.)

Abstract: This work assesses the use of different solar heating integration configurations and heating storage solutions for three different agri-food industries located in southern Europe. TRNSYS is employed to model different Solar Heat for Industrial Process (SHIP) integration options and to quantify the solar thermal share with respect to the overall thermal demand, as well as to estimate the avoided consumption of fuels and CO_2 emissions in the existing boiler units as a result of the solar system integration. The SHIP integration is complemented with the evaluation of selected phase-change materials (PCM) to promote latent heat storage under the specific conditions of the considered agri-food demo sites and solar irradiation characteristics. The arrangement of flat-plate solar collectors coupled with latent heat storage was found to enhance the yearly averaged solar share of the SHIP solutions, reaching 13% of the overall thermal demand for an average Spanish winery demo site. Furthermore, the estimation of the gross solar heat production for a mid-size Italian spirits distillery yielded 400 MWh/y, leading to annual fossil fuel savings of 32 tons and yearly avoided CO_2 emissions of up to 100 tons. Similarly, the SHIP integration model for an average French charcuterie predicted a 55% solar share of the thermal demand required for plant cleaning purposes, resulting in roughly 50 tons of CO_2 emissions avoided per year. The estimated payback period (PBP) for the Italian spirits demo case under the current economic scenario is below 9 years, whereas the PBP for the other demos does not exceed the expected lifetime of the solar plants (25 years).

Keywords: solar thermal; renewables; PCM; solar heating; industrial heating; solar share

Citation: Guillen-Angel, J.; Julian, I. Evaluation of Technical Feasibility of Solar Heat Integration in Agri-Food Industries. *Processes* **2023**, *11*, 696. https://doi.org/10.3390/pr11030696

Academic Editors: Carlos Herce, Benedetta de Caprariis, Yolanda Lara and Paola Ammendola

Received: 30 November 2022
Revised: 30 January 2023
Accepted: 17 February 2023
Published: 25 February 2023

1. Introduction

Despite it being accepted that solar thermal can provide a large amount of the industrial heat demand, the actual deployment levels remain very low or even insignificant. As an example, roughly 95 solar thermal plants with a total capacity of 41 MW_{th} were installed globally for the food industry up to 2020 [1]. The main challenges that are tapping its potential are related to (a) Solar Heat for Industrial Process (SHIP) economic competitiveness and (b) the complexity of the integration in existing industrial processes [2].

On one hand, the SHIP costs are highly dependent on the process temperature level, the heat demand continuity, the project size and the level of solar radiation. On the other hand, the integration of solar heating within industrial environments with high energy demand requires the inclusion of storage systems to decouple generation and consumption of energy, therefore, ensuring heating is available throughout the day.

However, the recent geopolitical events resulting in the drastically increased price of fossil fuels and its unpredictable fluctuation for the coming period, coupled with the global commitment towards industrial processes decarbonization, open a window for the penetration of this technology for a more sustainable industrial production.

Two types of solar thermal collectors are currently available: non-concentrating (or stationary) and concentrating. The former uses the same area for intercepting and absorbing solar radiation, whereas the latter has concave reflecting surfaces to intercept and focus the sun's radiation on a smaller receiving area, thereby increasing the radiation flux [3].

Non-concentrating units include flat-plate and evacuated tube collectors, which can deliver a maximum peak temperature up to 80 °C and 200 °C, respectively. Single-axis concentrating units, such as parabolic through and linear Fresnel collectors can, however, deliver temperatures as high as 400 °C. Finally, more advanced collectors, such as the two-axis concentrating units (parabolic dish or power tower receiver collectors), can deliver temperatures beyond 1000 °C. Examples of industrial processes requiring such high temperatures are steel, alumina, cement or lime production factories [4].

Compared to those, the heat requirements of industrial processes in the food and beverage industry are quite lower, often being the target temperature for the water/steam grid lines below 150 °C. Typical heat-demanding processes in the agri-food sector include drying, blanching, boiling, pasteurizing, smoking and sterilizing, apart from space heating or cleaning, for which thermal demand could be fully or partially satisfied with commercially available solar stationary collectors [5]. Further applications of such distillations (e.g., sugar refining) may require steam temperatures beyond 150 °C, for which the use of concentrating collectors may be more appropriate. A number of recent research works assess the potential and feasibility of solar integration in specific sectors, such as meat [6], beverage [7] or dairy industries [8]. In particular, García et al. [6] found that, in a medium-sized meat industry with energy demand close to 85 MWh_{th}/year located in a region with high irradiation, the profitability value of installing evacuated tube collectors for solar thermal integration purposes rises up to 1.1, the estimated payback period being under 9 years, the solar share higher than 50% of the overall thermal requirements and the annual energy bill reduction over 40%. Similarly, Holler et al. [7] found that the arrangement of parabolic trough collectors for steam generation at 180 °C at a beverage industry located at a mid-latitude region could potentially provide a solar share in the range of 17–23%, with a thermal output up to 2 MW, being a levelized cost of solar steam generation of 55–60 EUR/MWh. Furthermore, Sharma et al. [8] attempted to estimate the SHIP integration potential in milk processing plants throughout India, finding that the equivalent solar collector area requirement for process heating in the dairy industry is in the range of 1.54–1.83 million m^2, with an average solar share estimated in the range of 0.18–0.32, the potential yearly CO_2 emissions mitigation being in the range of 32–144 thousand tons.

A recent review paper [1] summarizes these economic feasibility studies and presents a literature survey on the installed solar collectors for food, dairy and meat product manufacturing and processing, as well as for fruit and vegetable preserving. The common feature of the installed collectors is the maximum temperature requirement of the industrial process where they are installed, which is below 150 °C. This review paper also reveals that the estimated payback period and levelized cost of energy for SHIP integrations in tropical locations are below 8 years and 90 EUR/MWh_{th}, respectively. So far, these sources provide a holistic techno-economic assessment of the solar thermal integration based on different solar collector technologies and usually include a rough estimation of economic indicators, such as payback period or reduction in the annual energy bill. Nevertheless, given the current volatile market price of electricity and raw materials, the techno-economic estimations are fraught with uncertainty and may easily become obsolete. As such, the most valuable indicator to assess the solar thermal integration potential at each agri-food industrial processing site is the solar share, i.e., fraction of the overall thermal demand for the industrial process provided by the solar thermal plant. The solar share (SS) depends on many factors, such as thermal demand profile, collector technology, available area for the installation of solar collectors, local irradiance or the possibility to store the generated solar heat. For this reason, although some general guidelines can be inferred regarding the applicability and potential of SHIP integration in the agri-food sector, the enormous variability of size and location of such industrial activities requires a case-by-case analysis to be conducted in order to assess its specific potential.

In this framework, this work presents a technical feasibility study on the SHIP integration in agri-food industries in southern Europe, targeting the most favorable scenarios for its implementation. The three selected demo sites are a winery company located in

Spain, a spirits distillation site in Italy and a charcuterie in France (Figure 1). All of them represent locations with relatively high solar radiation rates, having industrial processes with temperatures below 250 °C and being very energy-intensive and fossil-fuel-dependent. Specifically, the purpose is to explore different solar thermal integration alternatives to minimize fossil fuel consumption, CO_2 emissions and maximize solar share.

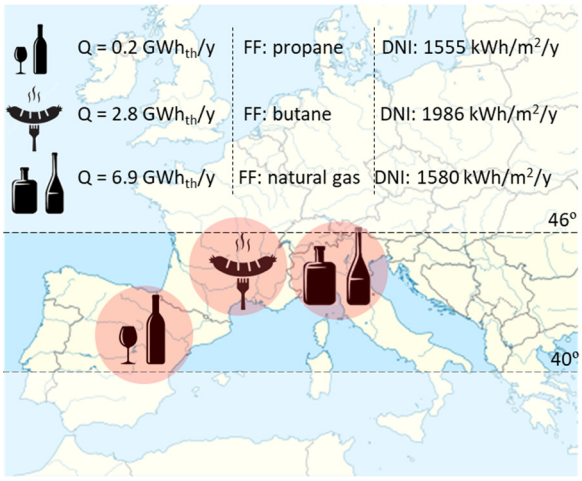

Figure 1. Location, agri-food sector, yearly heating demand, currently employed heating source and direct normal irradiance (DNI) for the three demo cases analysed in this study: Spanish winery, Italian spirits distillery and French charcuterie.

In order to meet the characteristic thermal demand (flow and temperature) of each demo site, different solar technologies and storage systems have been simulated, including evacuated tubes and ultra-high vacuum flat-plate collectors, as well as phase-change materials (PCM) as advanced heat storage solutions.

The coupled use of latent heat storage and solar thermal technologies has already been reported with different degrees of success for both air and water heating [9–20], as well as for absorption cooling system applications [21]. However, the vast majority of technology-coupling attempts refer to residential applications. This paper, thus, emerges as the first techno-economic assessment dealing with the combined integration of solar thermal and latent heat storage (based on PCM) into real existing agri-food industrial processes.

Latent heat storage (LHS) emerges as an alternative that combines innovation and a promising performance in comparison with sensible heat storage. Typically, PCM, as latent heat storage vectors, may provide energy densities up to 280 kJ/kg [22], which represents around three to four times higher energy density than that delivered by sensible heat systems [23]. As a result, the LHS based on PCM may potentially provide a significant increase in the thermal storage capacity and system volume reduction. Besides, LHS features the ability to provide the stored energy at a nearly constant temperature during the phase changing.

Regarding the technology cost, sensible heat thermal energy storage (TES) systems are rather inexpensive, as they basically consist of a tank for the storage medium. However, the container of the storage material requires effective thermal insulation; otherwise, it would be rapidly discharged. In general, the cost of a PCM-based system ranges between 0.1 and 10 EUR/kWh in cases of low and medium temperatures, while it is increased up to 70 EUR/kWh for higher temperature [24]. Considering the overall system, including the cost of container, heat exchanger, insulation and other surrounding components, a suitable range to be considered as a completely economically feasible alternative should be set at 40 EUR/kWh.

One of the most used configurations is based on a conventional water tank, with several double-port connections and optional internal heat exchangers, integrating PCM modules as depicted in Figure 2a. The PCM modules can have different forms and shapes

depending on the encapsulation (usually cylindrical, spherical or rectangular). The hot water coming from the solar system flows inside the tank and the PCM modules absorb the heat and store it until the demand period, when the heat transfer fluid is discharged in the SHIP process for multiple purposes (production processes, climatization, space heating and/or cooling, cleaning tasks, etc.). An example with cylindrical modules and a double port connection with no heat exchanger is shown in Figure 2b [18]. Figure 2c shows an alternative hybrid option with internal heat exchanger and PCM integrated in smaller capsules located in a vertical position close to the upper base of the tank [25]. The volume fraction of the PCM represents in this case less than 25% of the total tank volume.

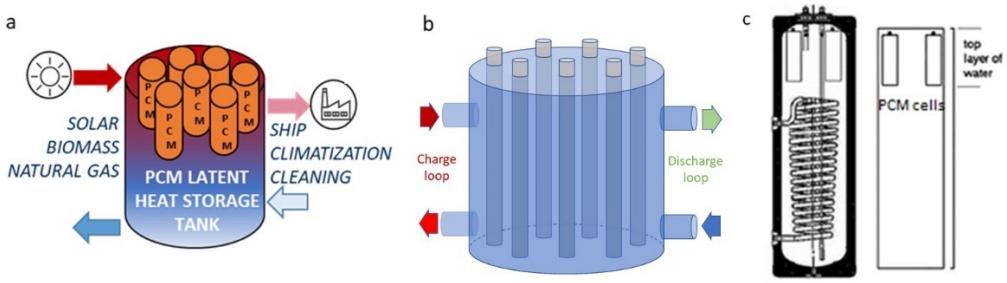

Figure 2. (**a**) Diagram of PCM-TES integration; (**b**) water storage tank with cylindrical PCM modules inside (adapted from [18]); (**c**) hybrid heat storage tank with internal heat exchanger coil and PCM capsules (with copyright permission from Elesvier) [25].

The encapsulation of PCM within storage tanks is one of the most expensive shares in the overall system; hence, it is important to optimize the design to avoid unnecessary costs. In these configurations, the following variables can be easily modified to adapt the volume and the resulting heat transfer area: number of cylindrical PCM modules introduced in the tank, height, diameter and location.

Regarding the SHIP integration promoted by PCM-TES, typically the hot water from the solar installation flows into the storage tank, in which the set of PCM modules absorb and store the heat. Therefore, the key variables that determine the heat transfer area, tank volume and integration efficiency are (1) number of PCM modules, (2) cartridge height, (3) cartridges diameter and (4) location within the tank.

The SHIP integration schemes adopted along this research work are intended to attain the highest possible solar thermal share with respect to the overall thermal demand of the processing plants.

2. Simulation Models

The assessment of the different SHIP integration configurations was conducted using the transient simulation software TRNSYS. Each solar heat model definition requires a number of unit models and input parameters to be defined, ranging from the irradiation and weather data set from the selected locations, the monthly distribution of the thermal demand by the industrial process, as well as the most suitable process units and controllers among the available ones for the final application. Process unit types include solar collectors, heat exchangers, heat storage tanks, boilers, steam generators (if required) and variable speed pumps, whereas control units include differential and iterative feedback controllers. Ancillary utilities, such as data readers, integrators, plotters and unit conversion routines, are also required. The employed TRNSYS types and their roles are depicted in Figure 3.

"Input raw data" types are used to read weather and irradiance historical data at the selected location as well as to read historical production data files and incorporate the transient process demand conditions (temperature, pressure and flowrate) to the model. The "data customization" tools are intended to filter the raw input data, select specific fields, perform basic calculations between data sources, integrate signals and/or provide a time-discretized adaption of the available raw data. "Control" types help to keep the simulated system working under prescribed limits for different operating conditions as well

as to enhance numerical convergence. The "output data monitoring" types are intended to monitor the online transient simulation results and to store specific simulated parameter data on demand. Finally, the "SHIP process units" represent the numerical models of the different operating equipment in the solar field. These include a sort of solar collectors, heat exchangers, heat storage and buffer tanks, boilers, variable speed pumps and PCM tanks.

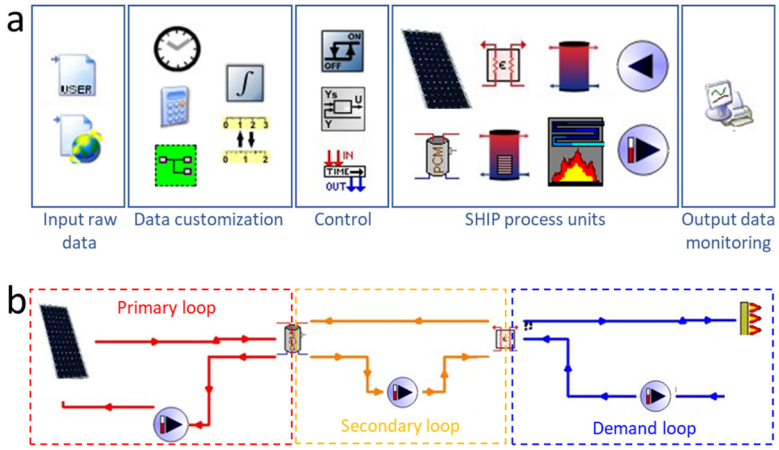

Figure 3. (**a**) TRNSYS types and their corresponding icons sorted by role; (**b**) typical three-loop circuit adopted for the simulation of the different SHIP integration options along this work.

Regarding PCM tank modeling, the latent thermal storage tank was simulated using Type 840, a multi-node storage model developed by the Institute of Thermal Engineering in Graz to be used directly within Trnsys environment [18]. The storage volume is divided into a user-defined number of horizontal segments (nodes), each characterized by its enthalpy and mass of fluid in which an energy balance is solved at every timestep, leading to an evolution of the enthalpy. Following this, temperature calculated as enthalpy density is considered as a continuous and invertible function of temperature [26].

The simulation sketch adopted to simulate the SHIP integration in the different demo sites consists in a three-loop circuit containing a "primary" (solar) loop, a "secondary" (storage) loop and a "demand" loop.

The former holds the solar collector fed with glycol water as heat transfer fluid, weather data definition, pumping equipment and a heat exchanger. Further features include a control system to limit the outlet temperature of the collector up to a certain prescribed threshold value, a differential controller for the high-temperature fluid pump and a delayed output device to facilitate numerical convergence in case of fast and sudden change of fluid flow thermal and/or pressure conditions.

The secondary loop holds the heat storage tank (heat buffer) that transfers the fluctuating energy flow from the solar radiation into a hot water circuit, a heat exchanger to provide the solar field energy to the process demand loop and pumping equipment. Similarly, this circuit incorporates control loops to tune the relative fluid flowrate between primary and secondary to prevent fluid overheating, as well as a delayed output device for convergence purposes.

Finally, the demand loop integrates the demand definition file, the water/steam pumping module, the cold flow section of the heat exchanger and a conventional boiler system. The demand definition is computed using transient mass flows and temperatures from the process streams based on historical and seasonal operation data at the analyzed demo sites. The role of the conventional boiler is to provide the required temperature demand whenever it is not reached by the solar field. The eventual consumption of fossil fuel to run the boiler and reach the demand flow temperature is, thus, computed to evaluate the solar share according to Equation (1).

3. SHIP Integration Options and Case Study Description

3.1. SHIP Integration

The solar integration application can be generalized as a set of connected units and equipment in an assembly similar to that shown in Figure 4, which can be divided into a solar field set (i.e., collector loop + charge + storage) and an integration concept set (discharge + integration point + conventional process heat) [12].

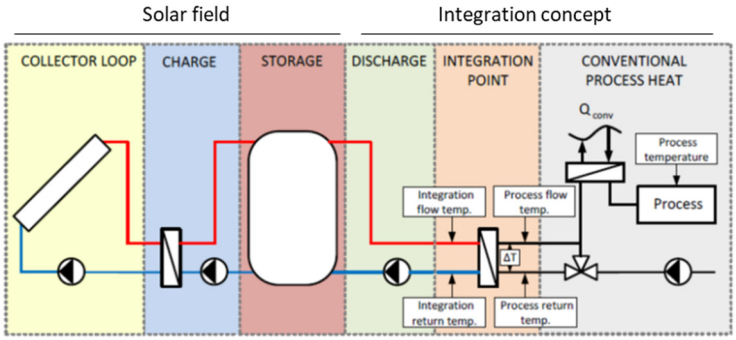

Figure 4. Block diagram of a typical solar thermal integration scheme in an industrial process [12].

Typically, the solar field can be arranged into four different configurations depending on the collector and fluid type. The high-temperature fluid may be driven either to a heat exchanger or directly to a buffer tank. The former prioritizes the collector loop efficiency and provides the flexibility to use different media in the collector field and storage. The second represents a cheap and robust solution, although the collector fluid becomes the storage fluid and this may eventually constrain the heat storage capacity enhancement that other fluid formulations and/or phase-change materials can provide. Another possibility is to use the liquid fluid solar field for indirect steam generation, in which the high-temperature outflow would be conducted to a steam generator. The resulting steam could be either injected to the general steam supply line or directly to the target process [12]. The solar field applications dealing with liquid water heating and/or indirect steam generation use typically evacuated tubes or high-vacuum flat solar collector technologies. In contrast, those requiring large steam flows at high temperatures use concentrated collectors (e.g., Fresnel-type) for the direct steam generation. The latter collectors preheat, evaporate and super-heat the heat transfer medium (essentially water) to the desired temperature and the generated steam can be immediately sent to the supply line or employed in the process. However, the high pressures that are typically attained in the system require thicker and more expensive piping, as well as a demanding process control [12].

Regarding the integration concepts, there are two general options: integration at supply or at process level. The first involves, for instance, the preheating of the boiler feed water, preheating of the make-up water or the heating of the supply heat storage.

The second includes a wide variety of options, such as the heating of process vessels, process media (e.g., product, fresh water and drying air) and process heat storage. A list of the most convenient solar integration configurations in industrial processes can be found in the Task 49 document "Solar Process Heat for Production and advanced applications" published by the Solar Heating and Cooling Programme of the International Energy Agency [12].

In this regard, the SHIP integration schemes adopted in the three demo sites are intended to attain the highest possible solar thermal share with respect to the overall thermal demand of the processing plants. The selected integration concepts for each particular demo have been assessed by both SHIP facilitators and end users, taking into account the characteristics of the thermal demand distribution, the solar field availability and the intrinsic potentials of each solar region.

In order to assess the techno-economic feasibility of the explored SHIP integrations, a series of technical and economic Key Performance Indicators (KPI) have been defined.

These are yearly averaged solar share, avoided use of fuels, reduction in CO_2 emissions in the existing boiler units, payback period and internal rate of return (Equations (1)–(5)). In Equation (1), $\dot{Q}_{solar}$ represents the thermal power than can be potentially delivered by the solar plant, whereas $\dot{Q}_{fuel,0}$ refers to the thermal power required by the industrial process, which is currently fully supplied by fossil fuel combustion. In Equation (2), $\dot{m}_{fuel,0}$ represents the mass flow of fossil fuel required to fulfill the thermal requirements of the industrial process without SHIP integration, whereas $\dot{m}_{fuel,f}$ is the remaining mass flow of fossil fuel required to reach the thermal demand of the process after integrating a solar thermal unit. Similarly, $\dot{m}_{CO_2,0}$ and $\dot{m}_{CO_2,f}$ in Equation (3) refer to CO_2 emissions by fossil fuel combustion in the absence and presence of auxiliary solar thermal power, respectively. In Equation (4) $CAPEX_{total}$ refers to the initial investment cost for the solar thermal plant, S_{total} are the yearly savings related to CO_2 emissions reductions and avoided fuel consumption and $OPEX_{total}$ refers to the yearly operational expenditures of the solar plant.

$$\%\ Solar\ share = \frac{\dot{Q}_{solar}}{\dot{Q}_{fuel,0}} \tag{1}$$

$$\%\ Avoided\ fuel\ consumption = \frac{\dot{m}_{fuel,0} - \dot{m}_{fuel,f}}{\dot{m}_{fuel,0}} \tag{2}$$

$$\%\ CO_2\ emissions\ reduction = \frac{\dot{m}_{CO_2,0} - \dot{m}_{CO_2,f}}{\dot{m}_{CO_2,0}} \tag{3}$$

$$Payback\ period\ (PBP) = \frac{CAPEX_{total}}{S_{total} - OPEX_{total}} \tag{4}$$

3.2. Italian Spirits Distillery

The spirits distillation site based in the north area of Italy is subjected to a direct normal irradiance (DNI) of 1580 kW/m^2/y and a global horizontal irradiance (GHI) of 1657 kW/m^2/y, measured at an inclination of 35°. Its global heating demand is around 6.9 GWh$_{th}$/y. A relevant heat fraction out of it is employed for the distillation bottle warming and sanification, which uses steam at 135 °C and 3 bar. Currently, both steam boilers and a combined heat and power plant (CHP) address the required steam needs. The available area for the arrangement of solar collectors is roughly 600 m^2 and the estimated gross heat production per year is around 350 MWh$_{th}$.

The proposed solution to tackle the SHIP integration in this demo-site consists of the seasonal use of solar thermal energy for different purposes. During the winter season, in which the solar collectors would receive lower radiation, the solar thermal field would be employed for space heating, while, in summer, it would be employed for indirect steam generation. Table 1 summarizes the demand requirements at the two seasons.

Table 1. Seasonal thermal demand for the current SHIP integration scheme in the Italian spirits industry.

Season	Stream Type	Steam Flowrate $\dot{m}$ (kg/h)	Process Temperature T_p (°C)	Return Stream Temperature T_r (°C)	Process Pressure P_p (bar)
Winter period	Hot water	700	90	70	4
Summer period	Steam	18,000	170	160	10

This dual-integration scheme is envisioned to be carried out using a high-vacuum flat solar thermal panel technology attached to a steam generation unit. These panels can capture 100% of sunlight, both direct and diffuse, while exhibiting minimal thermal losses by convection and no degradation over time, delivering exceptional efficiency. Moreover, they can deliver temperatures up to 200 °C, thus, being suited for both district heating and industrial process purposes.

The simulation model deployed for the indirect steam generation application considers a flat solar collector panel module (type 432) adapted to account for the characteristic properties of the high-vacuum flat panels. With the aim of considering realistic figures for the collector performance, a commercial high-vacuum flat panel from TVP Solar [27] was selected as a reference collector for the simulation study. Its power performance curve is described by a zero loss efficiency at normal incidence of 0.737, zero collector heat loss coefficient of 0.504 W/m^2K and the temperature difference dependence of the heat loss coefficient of 0.006 W/m^2K^2 [28]. The proposed solar integration scheme is depicted in Figure 5.

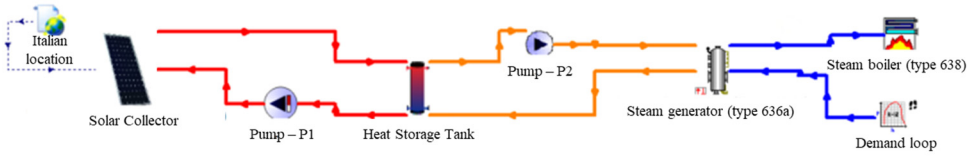

Figure 5. Solar integration scheme for the Italian spirits distillation site based on the use of high-vacuum flat panels for the indirect steam generation application along the summer period. The solar plant includes a buffer tank.

The model considers that the fluid of the primary circuit (red line) is a 30 wt.% glycol–water mixture. The outlet hot mixture from the solar collector enters the upper section of a vertical 20 m^3 heat storage tank (HST), in which it exchanges heat with the colder water volume recirculated from the secondary circuit (orange line). Both primary and secondary circuit fluids are pumped by adaptive flow pumps P1 and P2. The hot water from the HST is fed to a steam generator (Trnsys type 636a), in which the process water from the condensates tank (blue circuit) becomes boiled. The steam boiler connected in series with the steam generator helps to reach the required steam temperature to feed the steam grid. The monthly averaged heat demand from the Italian plant corresponding to the 2021 period was considered as input demand to run the simulations. Analogously, the irradiation data for the specific Italian site location along 2021 were used as weather input data.

3.3. Spanish Winery

The winery based in Spain is subjected to a DNI of 1555 $kW/m^2/y$ and a GHI of 1641 $kW/m^2/y$, measured at an inclination of 35°. Its global heating demand is around 0.2 GWh_{th}/y. The available collector area is around 110 m^2 and the potential yearly solar heat production is roughly 50 MWh_{th}.

The SHIP integration envisioned for the winery considers the preheating of the condensates tank using latent heat storage to enhance the storage capacity and reduce the transient temperature fluctuation as a result of the irradiation intermittency. The preheated water will be subsequently driven to the boiler, in which the required process temperature will be reached. The proposed integration scheme is depicted in Figure 6. Analogously to the Italian spirits case, three circuits are considered for the solar integration. The considered solar collector is an evacuated-tubes-type collector. With the aim of pursuing a realistic simulation based on the collector performance of a commercial unit, a Vitosol 300-TM vacuum tube collector from Viessman was considered [29]. Its main characteristics are (a) zero loss efficiency at normal incidence: 0.481; (b) incidence angle modifier for the diffuse radiation: 0.974; (c) zero collector heat loss coefficient: 1.118 W/m^2K and (d) effective heat capacity of the collector: 15,320 J/m^2K, among others [29]. The outlet stream from the collector is driven to an HST containing PCM cartridges for the hybrid sensible and latent heat storage. The secondary circuit provides the solar thermal energy to preheat the returned water from the process in the condensates tank prior to entering the boiler.

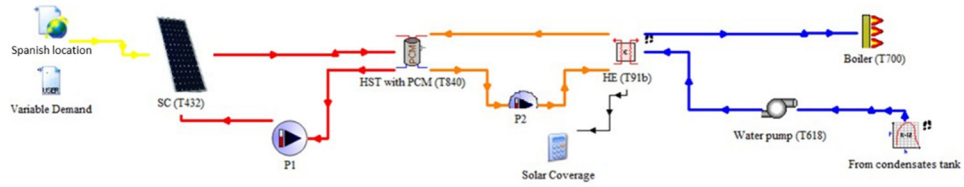

Figure 6. Solar integration scheme for the Spanish winery demo site based on the use of Viessmann solar thermal collectors for hot water generation and a heat storage tank with PCM.

Different from other agri-food industries, wineries have a strongly seasonal thermal energy demand, since the characteristic malolactic fermentation and related activities typically carried out during autumn cover nearly 45% of the yearly heating and cooling requirements [30]. As such, the solar share in this sector may be strongly fluctuating along the different seasons.

In order to assess the role and performance of different PCM materials, various candidates with different phase-change temperature as well as different PCM cartridge arrangements within the heat storage tank were evaluated. The simulated conditions to assess the SHIP integration with latent heat storage at the Spanish winery are depicted in Table 2. The involved variables are (a) PCM type, (b) HST capacity and (c) PCM's volume fraction. The aspect ratio of the HST, i.e., height/diameter (H/d), was set to 1.75 for all simulations. Similarly, the outer diameter of the PCM tubes was set to 80 mm, the remaining variables being varied accordingly to meet the PCM's volume fraction and overall tank volume specifications.

Furthermore, additional case studies were simulated to evaluate the role of the exposed PCM's surface area, i.e., number of PCM tubes for a given PCM's volume fraction with respect to the total HST capacity (Table 3). For all these simulations, the total height and volume of the HST were set to 1 m and 4 m^3, whereas the HST volume fraction occupied by PCM was set to 30%.

The evaluated PCM are (1) a paraffin-based commercial "RT70HC" from RubiTherm [31], with a transition temperature of 72 °C; (2) a sodium acetate trihydrate coupled with expanded graphite composite (SA-Gr), which has a phase-change temperature of 58 °C [18]; and (3) a lauric-acid-based PCM (LA), for which transition temperature is 44 °C. All PCM transitions are in the range of temperatures expected at the heat storage tank, given the installed capacity (2 m^3), solar collector area (110 m^2), yearly distribution of heat demand and solar irradiation at the plant location. The temperature-dependent evolution of the heat storage enthalpy and heating-cooling hysteresis for each material is depicted in Figure 7.

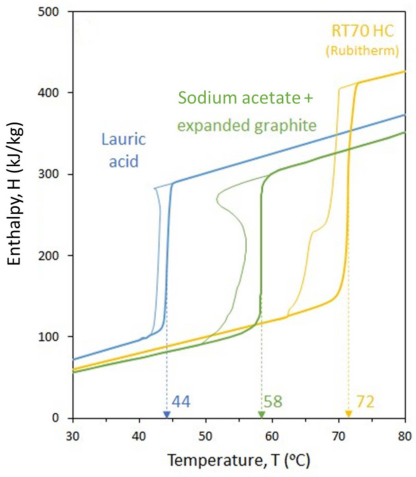

Figure 7. Characteristic temperature-dependant heat storage enthalpy of the three considered PCM for the simulation of the PCM-based heat storage tank as an alternative configuration of the SHIP solution adopted in the Spanish winery.

Table 2. Full factorial design of experiments matrix to evaluate the effect of HST volume, PCM type and PCM volume fraction on the solar share for the winery demo site.

#	HST Volume (m^3)	PCM Type -	PCM Volume (%)	d_{HST} (m)	H_{HST} (m)	No. PCM Modules	PCM Surface (m^2)
1	1	-	0%	0.9	1.6	0	0.0
2		RT70HC	10%			13	5.2
3			20%			26	10.4
4			30%			39	15.6
5		SA + graphite	10%			13	5.2
6			20%			26	10.4
7			30%			39	15.6
8		Lauric Acid	10%			13	5.2
9			20%			26	10.4
10			30%			39	15.6
11	2	-	0%	1.1	2.0	0	0.0
12		RT70HC	10%			20	10.2
13			20%			40	20.4
14			30%			60	30.6
15		SA + graphite	10%			20	10.2
16			20%			40	20.4
17			30%			60	30.6
18		Lauric Acid	10%			20	10.2
19			20%			40	20.4
20			30%			60	30.6
21	4	-	0%	1.4	2.5	0	0.0
22		RT70HC	10%			32	20.4
23			20%			64	40.7
24			30%			96	61.1
25		SA + graphite	10%			32	20.4
26			20%			64	40.7
27			30%			96	61.1
28		Lauric Acid	10%			32	20.4
29			20%			64	40.7
30			30%			96	61.1

Table 3. Design of experiments to evaluate the effect of the exposed PCM tubes surface area for a given HST geometry (H_{HST} = 1 m, V_{HST} = 4 m^3) and PCM tubes volume fraction (30%).

#	PCM Type	No. PCM Modules	PCM Tube Surface (m^2)
1	-	0	0.0
2	RT70HC	4	10.0
3		16	16.9
4		64	30.8
5	SA + graphite	4	10.0
6		16	16.9
7		64	30.8
8	Lauric Acid	4	10.0
9		16	16.9
10		64	30.8

3.4. French Charcuterie

The charcuterie based in France is subjected to a DNI of 1986 kW/m^2/y and a GHI of 1285 kW/m^2/y, measured at an inclination of 35°. Its global heating demand is around 2.8 GWh$_{th}$/y. The available collector area is around 1600 m^2 and the potential yearly solar heat production is roughly 1085 MWh$_{th}$.

In order to integrate the solar heat, the configuration envisioned for the factory lays in the preheating of cold water at 8 °C from the grid to provide water at 60 °C to feed the hot-water grid. The preheating of the cold-water flow may serve to (a) reduce the energy consumption of the heat pump that currently keeps two 100 m^3 tanks at 60 °C or (b) reduce the fuel consumption of an internally heated storage tank, namely Thermigaz tank, which holds 60 m^3 of hot water at 60 °C for processing area and slaughterhouse cleaning purposes.

The first configuration is shown in Figure 8a. In the proposed scheme, the solar plant may help to preheat the water from the grid up to certain temperature prior to entering the so-called "HE1-HP" heat exchanger. In this heat exchanger, the heat pump will provide the required energy input to reach 60 °C at the load side outlet.

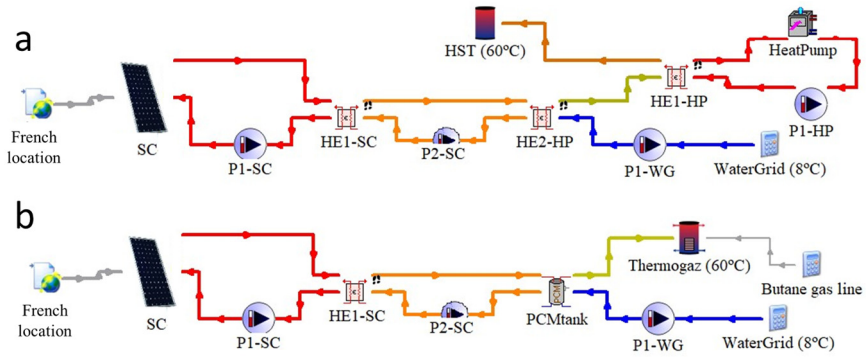

Figure 8. Solar integration configuration based on the preheating of the water from the grid to reduce (**a**) the energy consumption of the heat pump; (**b**) the fuel consumption in the Thermigaz tank, including PCM cartridges in the HST to modulate the tank temperature and increase heat storage capacity.

The second alternative configuration is aimed to accomplish the same water preheating role but, in this case, the solar energy is stored in a 60 m^3 pre-tank in order to minimize the temperature fluctuations of the system due to the solar intermittency (Figure 8b). The outlet stream from this heat storage tank is driven to a Thermigaz tank, in which the required heat to maintain the tank temperature at 60 °C is delivered by butane combustion. The simulated aspect ratio of the HST is H/D = 3, the tank height being 8.83 m. The nominal pump flowrate of both primary and secondary circuits is 15,550 kg/h. The analysis of the SHIP integration for the second configuration will be complemented with the assessment PCM as alternative latent heat storage options to reduce tank volume and increase solar share. To accomplish this, the simulated solar collector is a set of 510 ultra-high vacuum flat solar collector panels with an effective exposed area of 1.96 m^2 each. The characteristics of these collectors are described in Section 3.2.

4. Results and Discussion

4.1. Italian Spirits Distillery

As a first approach, a simulation was conducted to analyze the solar share that the potentially installed solar field can provide to the current combined heat and power (CHP) plant to feed the steam grid along the whole year. Figure 9a shows the monthly distribution of the heat demand by the distillery together with the monthly generated solar and CHP thermal power. Figure 9b highlights the simulated monthly solar share for this SHIP integration. As it is observed, the maximum solar share that this configuration can provide occurs along August, for which the low heat demand coupled with the high irradiation rate

result in an overall 17% of solar share. Nevertheless, the solar integration in the indirect steam generation is not envisioned as a suitable solution for the winter period, in which the solar share roughly rises up to 3%. This motivated the study of the seasonal solution described in Section 3.2.

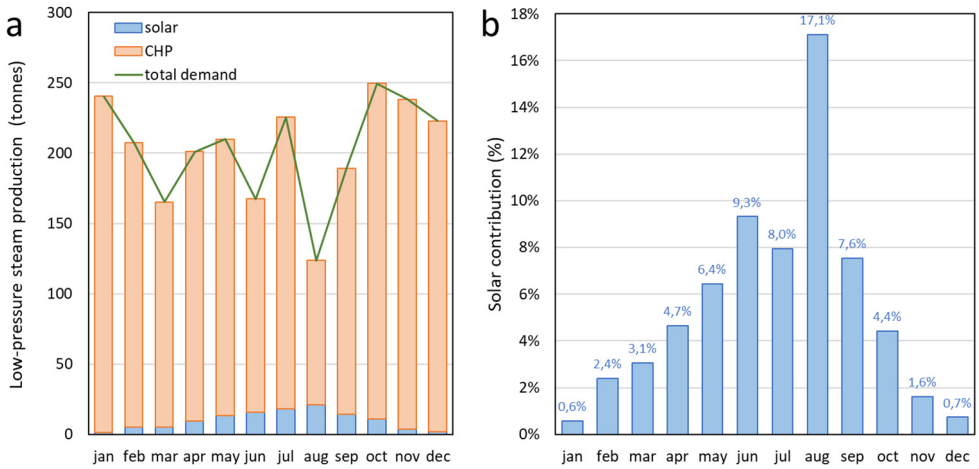

Figure 9. (**a**) Low-pressure steam demand profile and monthly distribution of accumulated steam production by the existing cogeneration (CHP) and the proposed solar plant at the Italian distillery; (**b**) monthly distribution of the solar contribution fraction to the low-pressure steam production.

As a result, further simulations concerning the SHIP integration for indirect steam generation were focused on the analysis of the solar share during the summer season. In particular, the solar field performance was compared either using an HST as heating buffer tank or a plate heat exchanger to deliver the solar heat directly into the steam generator. As Figure 10 suggests, the direct heat transfer from the solar loop to the steam generator via heat exchanger enhances the monthly averaged solar share with respect to that of the configuration employing HST. Essentially, for the proposed solar integration, the use of a heat exchanger increases the overall solar share nearly 24% within this period, with respect to that provided by the system using HST. These significant performance differences may be ascribed to the fact that the heat demand is substantially higher than the heat that the solar plant can supply, even at the highest transient irradiation periods in summer. Therefore, the use of a buffer tank to minimize temperature fluctuations derived from the intermittent irradiation does not become helpful to meet the demanding heat requirements of the process steam. Contrarily, the direct heat exchange from the primary circuit fluid to the steam generator loop helps to maximize the solar energy transfer and, more specifically, the peak solar thermal energy generated during intense irradiation periods.

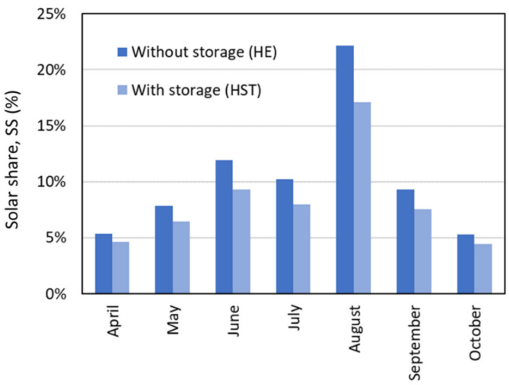

Figure 10. Role of the storage of heat on the monthly averaged solar share for the indirect steam generation assisted by solar thermal integration.

The study on the impact of solar heating over fuel consumption and CO_2 emissions indicated that 43,360 Nm^3 of natural gas was saved, accounting for 99.8 $t_{CO_2,eq}$ avoided per year for the configuration that maximizes the overall solar share, i.e., the system with direct heat transfer.

4.2. Spanish Winery

A parametric Trnsys simulation study was conducted based on the operating conditions described in Tables 1 and 2 to gain insight into the role of the integration of PCM in the storage tank volume reduction and storage capacity extension at the Spanish winery. Specifically, three promising PCM materials were evaluated (namely: SA-Gr, LA and RT70 HC), for which phase-change temperatures lay within the range of typical temperatures in the existing heat storage tank, given the installed solar collector area, tank capacity and process temperature demand. To illustrate this, Figure 11 shows the transient outlet fluid temperature at the heat storage tank in a simulated case study using a conventional tank without latent heat storage, highlighting the temperature range at which the proposed PCM implementation can play a role in the enhancement of heat storage.

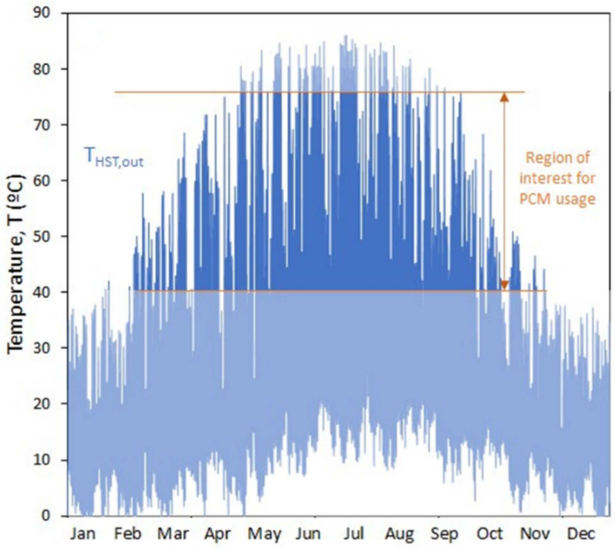

Figure 11. Simulated evolution of the outlet fluid temperature at the HST in the Spanish winery solar plant without using PCM.

As a previous point, Figure 12a shows the monthly thermal demand at the Spanish winery, expressed as propane consumption in the boiler (kWh/month), together with the overall solar thermal power production and solar share simulated using the SHIP configuration described in Figure 6. The simulation conditions are 110 m^2 of solar collector area, 4 m^3 of HST without latent heat storage and 1 m HST height. The propane consumption breakdown refers to historical monthly averaged thermal demand data of the demo site during 2018. This period was selected to illustrate the recent winery activity, since fuel consumption data during the global pandemic period are not as representative.

As can be observed, the heat demand becomes quite high along autumn (October–December) and drops drastically along summer. The simulation also reveals a significantly uneven monthly solar thermal power production and solar share. As Figure 12a shows, the monthly averaged solar share peaks up to 25% in June and July, whereas it hardly reaches 2% along December. Analogously, the maximum transient solar share is attained along the summer period, when the solar plant delivers around 60% of the process heat demand during mornings and afternoons (Figure 12b). Coupling the monthly average solar share and the process heat demand, the maximum solar thermal power production takes place in April (2.56 MWh/month), whereas the lowest power production occurs in

August (0.56 MWh/month) due to the very low process heating and cooling demand in that period. The annual average solar share of this particular SHIP integration is 12.76%.

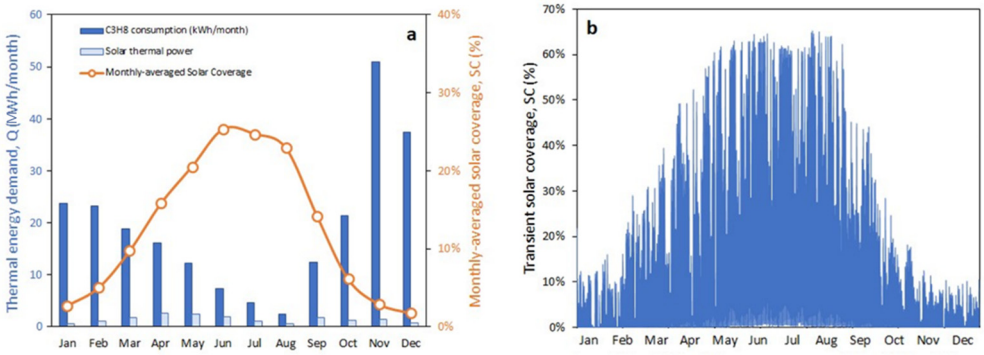

Figure 12. (**a**) Monthly distribution of the thermal energy demand and solar share in the Spanish winery demo site, including the amount of thermal energy delivered by the conventional boiler (C_3H_8 consumption expressed in kWh/month) and by the solar plant; (**b**) transient solar share.

Based on this preliminary result, the role of the latent heat storage on the annual solar share of the winery was evaluated. The simulated yearly solar share results are highlighted in Figure 13. As can be observed, the simulations suggest that the addition of PCM has a detrimental effect in cases where small HST are used, namely V_{HST} = 1 m^3 (Figure 13a). In contrast, this effect is reverted when higher tank volumes are employed, V_{HST} = 4 m^3 (Figure 13c). Interestingly, the lauric-acid-based PCM materials show the most noticeable HST performance improvement, working at V_{HST} = 2 m^3, whereas the sodium acetate trihydrate/graphite-based PCM outperforms the solar share of the other materials at V_{HST} = 4 m^3. A possible explanation for the observed trend is the fact that the annual average temperature in the HST is higher in the case of using a bigger tank, i.e., $T_{2\,m3}$ = 31.5 ± 16.0 °C, $T_{4\,m3}$ = 33.2 ± 16.0 °C (Figure 14). Actually, the time fraction at which the HST remains at temperatures between 40 °C and 50 °C (taking advantage of the latent heat storage of the LA-based PCM) is 12.0% for the 2 m^3 tank and just 8.1% for the 4 m^3 tank. The same circumstances apply to explain that SA-Gr outperforms LA in the case of V_{HST} = 4 m^3: the time fractions at which the tank remains at temperatures in the range 55 °C–65 °C (phase-change conditions for SA-Gr material) are 7.3% and 5.7% for V_{HST} = 4 m^3 and V_{HST} = 2 m^3, respectively.

In addition, Figure 13b,c reveal that the use of an increasing volume fraction of PCM has a detrimental effect on the solar share for the V_{HST} = 2 m^3 case, whereas it helps to enhance the share in the case of using V_{HST} = 4 m^3. Again, these opposed trends may be explained with the time period at which the tank temperature remains at a certain value that favors the phase change and, thus, the latent storage of the simulated PCM materials. As Figure 14d to Figure 14f suggest, the bigger the tank is, the larger the thermal inertia. Since the phase change of PCM substances requires some time to become effective, the longer the period that the tank remains at the target temperature range, the more significant an impact on the solar share will take place.

Figure 13d illustrates the effect of the exposed PCM cartridge surface to the water within the HST on the yearly average solar share. As expected, the greatest number of PCM modules employed at a constant PCM volume fraction within the tank (i.e., greatest surface area) results in the most enhanced solar share.

From the previous analyses, it can be concluded that the use of PCM for latent heat storage has a strong potential to provide enlarged thermal energy storage but the implementation of PCM-based HST units together with solar thermal plants needs to be conducted with care. For instance, its use in such a winery, for which energy demand is strongly fluctuating and seasonal, being most intense in the autumn–winter period, is probably not recommended. According to the case studies analyzed in this section, the impact of PCMs in the yearly averaged solar share is modest. The reason behind this is the intermittency

of the solar irradiation and, thus, the fact that the tank temperature lays most of the time outside the phase-change temperature range.

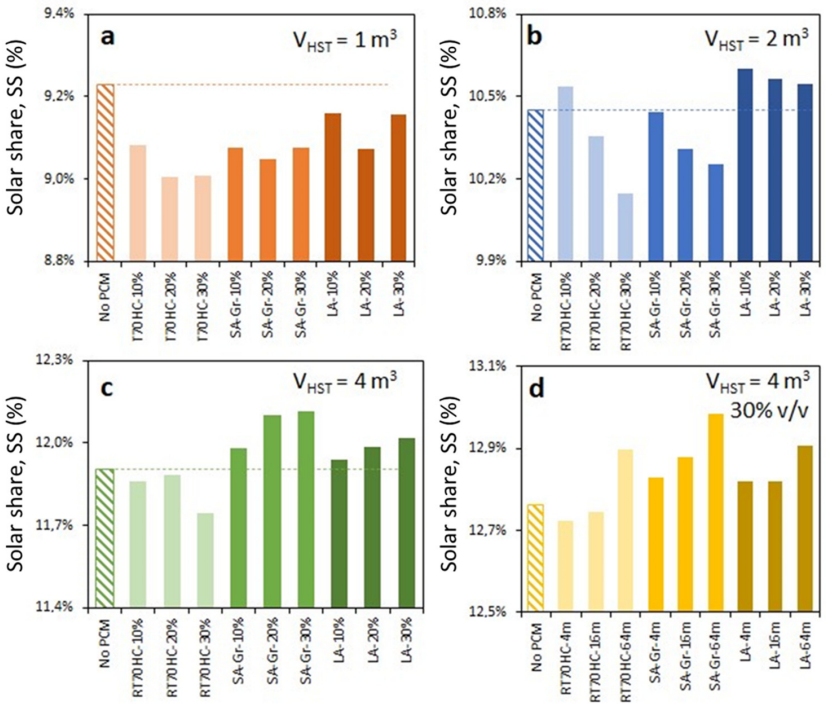

Figure 13. Role of the PCM type, HST volume, PCM volume fraction in the tank and number of PCM modules (heat exchange surface area) on the simulated annual solar share in the Spanish winery. Evaluation of the effect of PCM type and PCM volume fraction, keeping the aspect ratio of the HST constant, H_{HST}/D_{HST} = 1.75, and varying the tank volume: (**a**) V_{HST} = 1 m^3, (**b**) V_{HST} = 2 m^3, (**c**) V_{HST} = 4 m^3; (**d**) role of exchange surface area for V_{HST} = 4 m^3, H_{HST} = 1 m and 30% PCM volume fraction.

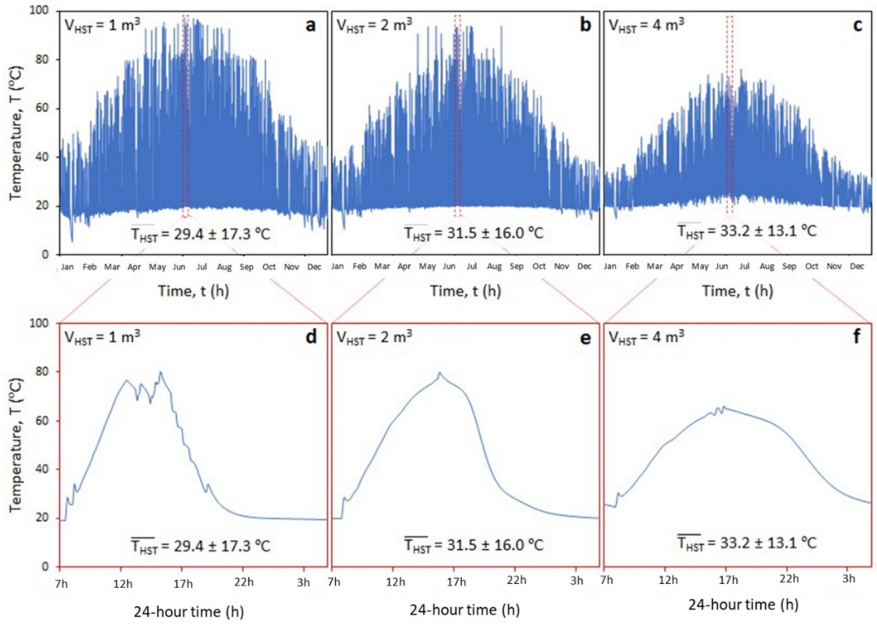

Figure 14. Simulated evolution of the HST outlet temperature for three winery case study scenarios without using latent heat storage based on PCM: (**a**) V_{HST} = 1 m^3, (**b**) V_{HST} = 2 m^3, (**c**) V_{HST} = 4 m^3. (**d**–**f**) represent a zoomed version of (**a**–**c**), showing the temperature evolution of a specific calendar day, namely 17 June.

In parallel to the solar share evaluation, the impact of PCM usage on the avoided CO_2 emission and reduction in fuel consumption were analyzed. It was found that 2054 kg of propane accounting for 6.15 $t_{CO_2,eq}$ per year were saved by considering the best solar thermal configuration. Here, "best" refers to the arrangement that provided the highest overall solar share, regardless of economic implications of latent heat storage implementation.

4.3. French Charcuterie

The analysis of this configuration has a twofold purpose: (1) estimate the solar share and (2) evaluate the impact of PCM addition in the heat storage tank on the solar share, overall energy storage and attenuation of temperature fluctuation within the tank. For this latter purpose, sodium acetate trihydrate with expanded graphite (SA-Gr) was selected as the most suitable PCM material for this specific application, taking into account that its phase-change temperature lays in the range of the target demand temperature [6]. The simulated PCM cartridges occupy 30% of the total HST volume. They are arranged as 400 modules (80 mm diameter each) along the full tank height.

The Trnsys simulation results of the three alternative solutions adopted for the solar thermal integration in the charcuterie, namely preheating of the hot water grid line (1) and cleaning line without (2) and with latent heat storage (3), are summarized in Table 4. As simulations reveal, the yearly solar thermal energy delivered by the first integration configuration is nearly 222 MWh, which represents a yearly averaged solar share of 8.1%. Alternatively, the configurations that preheat the cleaning water deliver roughly 192 MWh per year using the same installed collector area. However, the resulting average solar share for this purpose is beyond 55% due to the lower thermal demand requirements of this process (Q_{demand} = 354 MWh/y). The transient evolution of both outlet HST temperature and solar share for the second configuration without using PCM tanks is presented in Figure 15a,b, respectively. These results suggest that the consumption of butane to keep the cleaning Thermigaz tank temperature at 60 °C may be drastically reduced along the year and practically eliminated along the summer period.

Table 4. Yearly average solar share and solar thermal energy production of the alternative configurations evaluated for the solar integration in the French charcuterie demo site.

Alternative Configuration	Tank Volume (m^3)	Solar Share (%)	Q_{solar} (MWh/y)	Q_{demand} (MWh/y)
#1	-	8.11%	221.8	2824.8
#2	60	55.66%	192.8	353.9
#3	60	55.53%	192.4	353.9

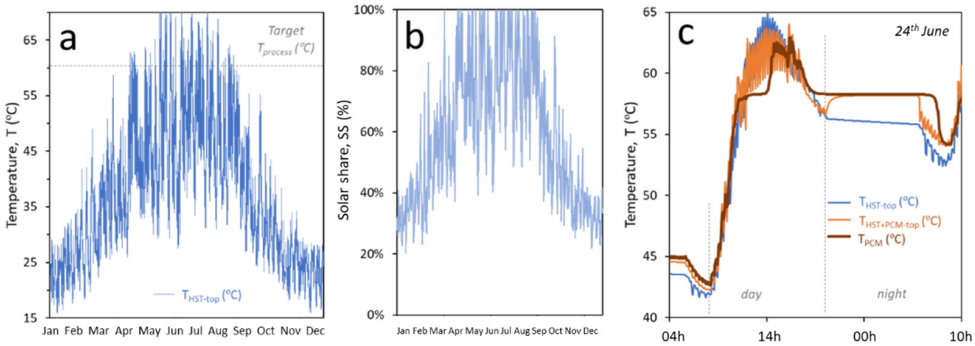

Figure 15. (**a**) Transient evolution of the HST top-side temperature in the second alternative solar integration configuration proposed for the French demo, using an HST without latent heat storage; (**b**) transient evolution of the solar share for the said configuration; (**c**) evolution of HST top-side temperature using HST without (blue) and with latent heat storage (orange), as well as transient PCM cartridge temperature along a specific calendar day, namely 24 June.

Regarding the use of SA-Gr PCM in the HST, a slightly detrimental effect is observed in terms of both overall thermal energy production and solar share. However, PCM addition has a relevant buffer effect, preserving higher tank temperatures along the night and limiting the temperature increase beyond 60 °C during irradiation peaks. This trend can be observed in Figure 15c. This figure shows the detailed temperature evolution along a summer day at the top side of an HST without (blue) and with (orange) PCM cartridges. The HST with PCM is able to provide 2 °C higher tank temperatures during the periods without solar irradiation, whereas it limits the highest tank temperatures close to 60 °C. Figure 15c also shows the temperature evolution of the PCM cartridges (brown line). Both the thermal inertia with respect to the top tank temperature and the phase-change phenomena (sudden temperature increase/decrease) can be clearly identified along the transient temperature evolution curve. As a result, the HST with SA-Gr PCM spends 205 h per year (7.2% of the time) at temperatures comprised between 55 and 60 °C, whereas the same tank without latent heat storage stays only 149 h per year (5.2% of the time) within this temperature range.

The assessment of both configurations over fuel consumption and CO_2 emissions indicated that configuration #1 leads to a reduction of 17,238 kg of butane, accounting for 46.2 $t_{CO_2,eq}$ per year, while the best arrangement of configuration #2, i.e., including latent storage based on SA-Gr, allows saving of 14,989 kg of butane, accounting for 40.2 $t_{CO_2,eq}$ per year.

4.4. Technical KPIs for SHIP Integration Assessment

This section aims to summarize the previous findings and to highlight the most promising simulation results for the three demo cases in terms of solar heat production. Table 5 shows the values of the KPIs (solar share, fuel saving and avoided CO_2 emissions) for the best scenarios among those evaluated for the Spanish winery, French charcuterie and Italian spirits distillery. Here, "best" scenarios refer to those that maximize the yearly average solar share for each demo, without taking into account the economic implications of each solar plant configuration. In the case of the Spanish winery, the highlighted configuration includes a PCM storage tank with 64 modules of sodium acetate trihydrate coupled with expanded graphite (30% v/v). Regarding the French charcuterie, an SHIP integration at the hot water grid line without latent storage was selected. Analogously, the most technically favorable case at the Italian spirits distillery was found to be the SHIP integration at the steam generation grid without thermal storage.

Table 5. Solar thermal production KPIs of configurations with highest solar share at every demo-site.

Case Study	Gross Solar Heat Production (MWh/y)	Solar Share (%)	Fuel Type	Fuel Saving (kg/y)	CO_2 Emissions Avoided ($t_{CO_2,eq}$/y)
Spanish Winery (SA-Gr 64 m 30% v/v)	26	13.0	Propane	2054	6.0
French Charcuterie (Config. #1)	222	7.8	Butane	17,238	51.0
Italian Spirits distillery	409	6.0	Natural Gas	32,217	99.7

Results suggest that, at the explored solar regions (DNI 1550–2000 kWh/m^2/y), the installation of solar fields at different industrial sites in the frame of the agri-food sector may cover roughly 10% of the overall thermal demand of the industrial processes. At the explored demo sites, the thermal demand is currently addressed using conventional boilers and/or CHP units fueled by fossil fuels, such as natural gas, propane or butane. By installing the proposed solar fields, for which collector area meets the available roof surface area at each facility, the fuel savings may be up to 32 tonnes of natural gas per year for a production site with a gross thermal demand of 6.9 GWh_{th}/y. Similarly, the avoided CO_2 emissions at such an energy-intensive industry may be up to 100 $t_{CO2,eq}$ per year.

Although these numbers correspond to three specific case studies at locations based in Southern Europe and may not be fully representative of the SHIP integration potential at the overall agri-food sector, they illustrate that a relevant decarbonization degree can be

accomplished. The potential benefits derived from the adoption of SHIP integration for the industrial processes will depend on the CAPEX and OPEX of the adopted solutions, as well as on the evolution of the fossil fuel price and legal restrictions and penalties applicable to CO_2 emissions.

As already anticipated in Section 1, existing literature data on SHIP integration in specific agri-food subsectors from which a fair comparison between current model predictions and available data can be made are scarce. Still, some conclusions can be drawn evaluating recent SHIP integration feasibility works for both meat processing [6] and beverage industries [7].

García et al. [6] analyzed a meat industry with an overall production of 230 t of pig-derivate products based in Madrid (Spain) and extrapolated the SHIP integration feasibility study to different capital cities in southern Europe. The overall thermal demand (around 85 MWh/year in the case of Madrid) is distributed into variable amounts of hot water in the range of 45–100 °C. The SHIP integration via evacuated tube collectors was evaluated to complement an existing electric boiler. Each collector has 2 m^2 net collecting area and 24 vacuum tubes. The optimized number of collectors to minimize the water heating expenditure over 20 years by SHIP integration at each location led to a solar share range between 34% (Berlin) and 53% (Rome). As a result, the theoretical thermal production of the solar field ranged from 510 kWh/y per m^2 of collector area in Berlin to 897 kWh/(y·m^2) in Athens. These theoretical solar thermal production values are similar to those considered in this work for the gross heat production capacity of the solar fields envisioned for an Italian distillery (583 kWh/(y·m^2)), Spanish winery (454 kWh/(y·m^2)) and French charcuterie (678 kWh/(y·m^2)), respectively.

Similarly, Holler et al. [7] found that the arrangement of parabolic trough collectors for steam generation at 180 °C at a beverage industry located at a mid-latitude region in Europe (Germany) could potentially provide a solar share of 17%, with a thermal output up to 2 MW, leading to a gross heat production capacity of 413 kWh/(y·m^2). Of course, the collector surface area refers here to the surface occupied by the arrangement of parabolic mirrors plus the required separation between consecutive units and not to the collecting tubes themselves. In any case, this estimation indicates that both solar thermal technologies (single-axis concentrating and non-concentrating collectors) lead to similar gross production capacities per collector area unit within the region of interest, i.e., southern and western Europe, which holds a large amount of low- and mid-size agri-food industries.

4.5. Economic KPIs for SHIP Integration Assessment

Although the current market price for raw materials and fossil fuels is highly fluctuating and, thus, any economic assessment of SHIP integration at any industrial sector is highly uncertain, Section 4.5 aims to bring some light into the profitability of the solar thermal integration in agri-food industries based on the three evaluated demo sites.

As depicted in Equation (4), the payback period can be calculated as the ratio between the investment cost, namely *CAPEX*, and the yearly cash flow, which is here considered as the sum of the avoided expenses of fuel use and the saved cost related to CO_2 emissions minus the yearly operating cost (*OPEX*) of the solar plant.

CAPEX refers to the total investment of the plant, considering both direct and indirect cost. Direct cost accounts for the acquisition and installation of the equipment, namely solar field, thermal storage and ancillary equipment, while indirect cost reports expenditures related to project engineering and development. The employed equation to calculate the overall *CAPEX* is depicted in Equation (5):

$$CAPEX_{total} = C_{sf} + C_{tes} + C_{aux} + C_{cont} \quad (5)$$

where C_{sf} represents the cost of solar collectors, C_{tes} refers to the cost of thermal storage, related to storage system and piping and C_{aux} is the cost of ancillary equipment, including instrumentation and control system. Moreover, a contingency cost related to total *CAPEX* is included to account for engineering related costs (C_{cont}). It has been assumed that the

cost of high-vacuum flat panels is around 450 EUR/m^2, while the cost of evacuated tubes collector is 400 EUR/m^2. These costs are based on estimations given by collectors' suppliers. C_{aux} has been assumed to be 5% of the overall *CAPEX* [32].

OPEX considers operation and maintenance of the solar plant for a typical year, therefore including fixed cost, such as labor and planned maintenance, and variable cost related to energy and utilities consumption (Equation (6)). Fixed cost is divided into power consumption by solar field (O_{sf}), power consumption by storage system (O_{tes}) and, alternatively, cost for maintenance and replacement of equipment (O_m), which is normally estimated for the whole solar plant as a percentage of *CAPEX*. In this work, it has been assumed that O_m can be estimated as 0.5% of the overall *CAPEX* per year [32], while O_{sf} can be assumed to be 1 EUR/(y·m^2) [33].

$$OPEX_{total} = O_{sf} + O_{tes} + O_m \quad (6)$$

Finally, the savings related to the integration of the solar system within an industrial plant are achieved by energy saved in the form of fuel or electricity (S_{fuel}) and greenhouse gases not emitted (S_{GHG}), whose cost is computed regarding the Emission Trading System in the EU (Equation (7)). For this purpose, it has been assumed that the costs of fossil fuel sources are 76.7, 85.9 and 85.9 EUR/MWh$_{th}$ for natural gas, butane and propane, respectively [34,35]. Analogously, the current price of CO_2 available by the Emissions Trading System of the European Union (EU ETS) is 85 EUR/t$_{CO_2,eq}$ [36].

$$S_{total} = S_{fuel} + S_{GHG} \quad (7)$$

Taking all these assumptions into account, Table 6 summarizes the economic indicators regarding overall CAPEX, yearly average OPEX, yearly savings related to fossil fuel and CO_2 emissions avoiding, as well as the estimated payback period for the solar plant configurations that maximize the solar share along the three evaluated demo cases. As can be observed, despite providing a relatively low solar share, the Italian spirits configuration with direct heat exchange (withou storage tank) minimizes the payback period among the evaluated cases, being it below 9 years. This value is very similar to that predicted by García et al. [6] for a Spanish meat processing plant.

Table 6. Economic indicators for the SHIP integration in the evaluated agri-food industry demo cases.

Demo Site	Fossil Fuel Savings (EUR/y)	CO_2 Emissions Avoided (EUR/y)	CAPEX (kEUR)	OPEX (EUR/y)	PBP (y)
Italian Spirits	37,605	8478	357.6	2384	8.2
French Charcutery	20,287	4337	454.4	3271	21.3
Spanish Winery	2263	513	41.8	359	17.3

However, the PBP of the SHIP integration solutions that involve the use of latent heating, i.e. French charcutery and Spanish winery, increases significantly. Nevertheless, the PBP for these technologies at the current economic scenario is still positive, as it lower than the expected lifetime of the solar plant (roughly 25 years).

5. Conclusions

This work analyzes the technical feasibility of the SHIP integration to partially decarbonize different agri-food SME industries along southern Europe. The proposed technologies allow the consumption of fossil fuels to be reduced by more than 10%.

An evaluation of potential alternative solutions for solar integration and thermal storage in the demo sites was performed from a theoretical level. This involved the analysis of a seasonal solar energy use for different purposes with and without heat storage for an Italian spirits distillery, the use of latent heat storage to increase the heat storage capacity and solar share in a Spanish winery and the coupled use of phase-change materials and the

parallel connected solar and conventional heating sources to fulfil the heating demand of the hot water grid at a French charcuterie.

Simulation results suggest that it is convenient to apply a seasonal energy use solution at the distillery, since the solar share for the indirect steam generation along autumn and winter for the available collectors' surface area, geographical location and installed solar technology hardly reaches 3%. Furthermore, it was shown that the installation of a heat storage tank as a fluid temperature buffer to minimize the effect of solar intermittency is detrimental for the overall solar share, as well as increasing CAPEX significantly, thus affecting payback period. The use of a plate heat exchanger to connect the primary (glycol water) and secondary fluid loops instead increases the solar share up to 24% and allows for a payback period of 8 years, the lowest of the three plants evaluated.

An assessment of the winery demo site resulted in a payback period below 20 years, despite seasonality of thermal demand, which is higher in periods of lower irradiance. Additionally, the energy efficiency and savings related to the use of latent heat-storage-based tanks was deeply investigated for the winery demo site. Beyond the theoretical potential of heat storage tank size reduction by using certain phase-change materials for a given thermal energy production (30% reduction using 30% PCM volume fraction in a 5 m^3 HST working at 90 °C), the simulations showed that the selection of suitable PCM for the characteristics of the solar plant is critical to guarantee a successful implementation of PCM-based HST. In particular, the thermal demand, tank size and heat production capacity of the installed heat collector determine the average temperature within the tank and the effectiveness of the PCM cartridges in storing the latent heat. As an example, lauric-acid-based PCM performed better for simulated 2 m^3 HST, whereas stearic-acid-based materials maximized the solar share using a 4 m^3 tank. In any case, it was shown that the integration of PCM in hot water tanks provides a peak power demand shifting and/or smoothing, mitigating the mismatch between solar energy supply and industrial process demand.

The alternative configurations proposed for the charcuterie involved the solar integration for the preheating of the water from the main grid at 8 °C in order to reduce the energy input of the installed heat pump and/or the fossil fuel consumption, which keep the hot water storage tanks at 60 °C. In the first scenario, the solar field is able to cover nearly 8% of the overall thermal demand, thus reducing the required energy input by the heat pump in 222 MWh/y; this configuration is expected to have a payback period of about 20 years. In the second scenario, the solar plant is able to provide 192 MWh/y, which represents nearly 55% of the total thermal energy demand for the charcuterie plant cleaning purposes. The addition of PCM in the HST helps to buffer the temperature evolution within the tank, storing latent heat during the nights and avoiding the appearance of HST temperature peaks beyond the demand temperature in intense irradiation periods.

As a general conclusion that spans all three evaluated configurations, solar heat has limited applicability in industries whose primary heat demand is in winter and the profitability of its implementation strongly depends on the inter-relation between (a) available irradiation at the SHIP integration place, (b) thermal demand characteristics (seasonal variability and target temperature) and (c) available surface for collectors' arrangement.

Author Contributions: The manuscript was written through contributions of all authors. J.G.-A. and I.J. have participated in (a) conception and design, (b) drafting and revising the article and (c) approval of the final version. All authors have read and agreed to the published version of the manuscript.

Funding: The project has received funding from the European Union's Horizon 2020 research and innovation programme under grant agreement No. 792276 (Ship2Fair).

Data Availability Statement: Not applicable.

Conflicts of Interest: The authors declare no conflict of interest.

Abbreviations

CAPEX	Capital expenditure
CHP	Combined heat and power plant
d	Heat storage tank diameter
DNI	Direct normal irradiance
GHI	Global horizontal irradiance
HE	Heat exchanger
H_{HST}	Heat storage tank height
HST	Heat storage tank
KPI	Key performance indicator
LA	Lauric acid
LHS	Latent heat storage
OPEX	Operational expenditure
PCM	Phase-change materials
Q_{demand}	Thermal demand
Q_{solar}	Solar thermal energy production
SA-Gr	Sodium acetate trihydrate with expanded graphite
SHIP	Solar Heat for Industrial Process
S_{total}	Yearly savings related to CO_2 emissions avoiding and fossil fuel consumption
SS	Solar share
TES	Thermal energy storage
V_{HST}	Heat storage tank volume

References

1. Ismail, M.I.; Yunus, N.A.; Hashim, H. Integration of solar heating systems for low-temperature heat demand in food processing industry—A review. *Papers* **2021**, *147*, 111192. [CrossRef]
2. Weiss, W.; Spörk-Dür, M. *Solar Heat Worldwide—Global Market Development and Trends in 2020-Detailed Market Data 2019: 2021 Edition*; AEE-Institute for Sustainable Technologies: Gleisdorf, Austria, 2021; Volume 37.
3. Carmona-Martínez, A.A.; Fresneda-Cruz, A.; Rueda, A.; Birgi, O.; Khawaja, C.; Janssen, R.; Davidis, B.; Reumerman, P.; Vis, M.; Karampinis, E.; et al. Renewable Power and Heat for the Decarbonisation of Energy-Intensive Industries. *Processes* **2023**, *11*, 18. [CrossRef]
4. Profaiser, A.; Saw, W.; Nathan, G.J.; Ingenhoven, P. Bottom-Up Estimates of the Cost of Supplying High-Temperature Industrial Process Heat from Intermittent Renewable Electricity and Thermal Energy Storage in Australia. *Processes* **2022**, *10*, 1070. [CrossRef]
5. Kumar, L.; Ahmed, J.; El Haj Assad, M.; Hasanuzzaman, M. Prospects and Challenges of Solar Thermal for Process Heating: A Comprehensive Review. *Energies* **2022**, *15*, 8501. [CrossRef]
6. García, J.L.; Porras-Prieto, C.J.; Benavente, R.M.; Gómez-Villarino, M.T.; Mazarrón, F.R. Profitability of a solar water heating system with evacuated tube collector in the meat industry. *Renew. Energy* **2019**, *131*, 966–976. [CrossRef]
7. Holler, S.; Winkelmann, A.; Pelda, J.; Salaymeh, A. Feasibility study on solar thermal process heat in the beverage industry. *Energy* **2021**, *233*, 121153. [CrossRef]
8. Sharma, A.K.; Sharma, C.; Mullick, S.C.; Kandpal, T.C. Potential of solar industrial process heating in dairy industry in India and consequent carbon mitigation. *J. Clean. Prod.* **2017**, *140*, 714–724. [CrossRef]
9. Ramya, D.; Gopal, S.R.; Sankar, S.M.U.; Tamilselvi, T.; Jagadish kumar, N.; Rinawa, M.L. Performance study on a mono-pass solar air heating system (MPSAH) under the influence of a PCM. *Mater. Today Proc.* **2022**, *69*, 934–938. [CrossRef]
10. Murali, G.; Mayilsamy, K.; Arjunan, T.V. An experimental study of PCM-incorporated thermosyphon solar water heating system. *Int. J. Green Energy* **2015**, *12*, 978–986. [CrossRef]
11. Sarbu, I.; Sebarchievici, C. A comprehensive review of thermal energy storage. *Sustainability* **2018**, *10*, 191. [CrossRef]
12. Hassine, I.B.; Helmke, A.; Heß, S.; Krummenacher, P.; Muster, B.; Schmitt, B.; Schnitzer, H. Solar process heat for production and advanced applications: Deliverable B2: Integration guideline. *IEA SHC Task* **2015**, *49*, 1–98.
13. Abokersh, M.H.; Osman, M.; El-Baz, O.; El-Morsi, M.; Sharaf, O. Review of the phase change material (PCM) usage for solar domestic water heating systems (SDWHS). *Int. J. Energy Res.* **2018**, *42*, 329–357. [CrossRef]
14. Sharma, A.; Chauhan, R.; Kallioglu, M.A.; Chinnasamy, V.; Singh, T. A review of phase change materials (PCMs) for thermal storage in solar air heating systems. *Mater. Today Proc.* **2021**, *44*, 4357–4363. [CrossRef]
15. Wheatley, G.; Rubel, R.I. Design improvement of a laboratory prototype for efficiency evaluation of solar thermal water heating system using phase change material (PCMs). *Results Eng.* **2021**, *12*, 100301. [CrossRef]
16. Medrano, M.; Yilmaz, M.O.; Nogués, M.; Martorell, I.; Roca, J.; Cabeza, L.F. Experimental evaluation of commercial heat exchangers for use as PCM thermal storage systems. *Appl. Energy* **2009**, *86*, 2047–2055. [CrossRef]

17. Wu, W.; Wang, X.; Xia, M.; Dou, Y.; Yin, Z.; Wang, J.; Lu, P. A novel composite PCM for seasonal thermal energy storage of solar water heating system. *Renew. Energy* **2020**, *161*, 457–469. [CrossRef]
18. Schranzhofer, H.; Heinz, A.; Streicher, W. Validation of a TRNSYS simulation model for PCM energy storages and PCM wall construction elements. Ecostock Conference 2006-Proceedings. 2006. Available online: https://www.researchgate.net/publication/251300668_VALIDATION_OF_A_TRNSYS_SIMULATION_MODEL_FOR_PCM_ENERGY_STORAGES_AND_PCM_WALL_CONSTRUCTION_ELEMENTS (accessed on 13 November 2022).
19. Belmonte, J.F.; Díaz-Heras, M.; Almendros-Ibáñez, J.A.; Cabeza, L.F. Simulated performance of a solar-assisted heat pump system including a phase-change storage tank for residential heating applications: A case study in Madrid, Spain. *J. Energy Storage* **2022**, *47*, 103615. [CrossRef]
20. Pelella, F.; Zsembinszki, G.; Viscito, L.; Mauro, A.W.; Cabeza, L.F. Thermo-economic optimization of a multi-source (air/sun/ground) residential heat pump with a water/PCM thermal storage. *Appl. Energ.* **2023**, *331*, 120398. [CrossRef]
21. Cerezo, J.; Lara, F.; Romero, R.J.; Hernández-Luna, G.; Montiel-González, M. Numerical Analysis of a Latent Heat Storage Using Plate Heat Exchanger for Absorption System Conditions. *Processes* **2022**, *10*, 815. [CrossRef]
22. Matuszek, K.; Kar, M.; Pringle, J.M.; MacFarlane, D.R. Phase Change Materials for Renewable Energy Storage at Intermediate Temperatures. *Chem. Rev.* **2023**, *123*, 491–514. [CrossRef] [PubMed]
23. Wang, R.Z.; Xu, Z.Y.; Ge, T.S. *1—Introduction to Solar Heating and Cooling Systems*; Wang, R.Z., Ge, C., Eds.; Woodhead Publishing: Cambridge, UK, 2016; pp. 3–12.
24. Alkan, C.; Sari, A. Fatty acid/poly(methyl methacrylate) (PMMA) blends as form-stable phase change materials for latent heat thermal energy storage. *Sol. Energy* **2008**, *82*, 118–124. [CrossRef]
25. Nkwetta, D.N.; Haghighat, F. Thermal energy storage with phase change material—A state-of-the art review. *Sustain. Cities Soc.* **2014**, *10*, 87–100. [CrossRef]
26. Voller, V.R. Fast Implicit Finite-Difference Method for the Analysis of Phase Change Problems. *Numer. Heat Transf. Part B Fundam.* **1990**, *17*, 155–169. [CrossRef]
27. TVP Solar, MT-Power Product Datasheet. 2017. Available online: https://www.tvpsolar.com/attach/MT-Power%20Datasheet%20(v4%20SK).pdf (accessed on 29 January 2023).
28. Buonomano, A.; Calise, F.; d'Accadia, M.D.; Ferruzzi, G.; Frascogna, S.; Palombo, A.; Russo, R.; Scarpellino, M. Experimental analysis and dynamic simulation of a novel high-temperature solar cooling system. *Energy Convers. Manag.* **2016**, *109*, 19–39. [CrossRef]
29. Viessmann, Vitosol 300-TM Product Datasheet Viessmann.Es. Available online: https://www.viessmann.es/es/edificios-de-viviendas/sistemas-de-energia-solar/colectores-de-tubos/vitosol-300tm.html (accessed on 18 November 2022).
30. Glaciem Cooling Technologies Pty Ltd., Thermal energy Storage for Renewable Energy Uptake in Wineries White Pap. ARENA Proj. Adv. Renewables with PCM Therm. Energy Storage. 2022. Available online: https://arena.gov.au/assets/2022/03/thermal-energy-storag-for-renewable-energy-uptake-in-wineries-white-paper.pdf (accessed on 13 November 2022).
31. Rubitherm, RT70 HC Data Sheet. 2020. Available online: https://www.rubitherm.eu/media/products/datasheets/Techdata_-RT70HC_EN_09102020.PDF (accessed on 13 November 2022).
32. De Santos López, G. Techno-Economic Analysis and Market Potential Study of Solar Heat in Industrial Processes A Fresnel Direct Steam Generation Case Study. Master's Thesis, KTH Royal Institute of Technology, Stockholm, Sweden, 2021.
33. EU H2020 research & innovation project SHIP2FAIR—Solar Heat for Industrial Process towards Food and Agro Industries commitment in Renewables; Deliverable 2.3: Key Performance Indicators to evaluate the integration of solar heating in industrial processes. 2018.
34. Eurostat, Gas Prices for Non-Household Consumers—Bi-Annual Data (from 2007 Onwards) 2022. Available online: https://ec.europa.eu/eurostat/databrowser/view/nrg_pc_203/default/table?lang=en (accessed on 11 January 2023).
35. European Commission, Energy Policy—Latest Prices LPG with Taxes. Available online: https://ec.europa.eu/energy/observatory/reports/latest_prices_with_taxes.pdf (accessed on 11 January 2023).
36. EU ETS, EU Carbon Price Tracker Ember-Climate.org. 2022. Available online: https://ember-climate.org/data/data-tools/carbon-price-viewer/ (accessed on 11 January 2023).